

Testing time-dependent density functional theory with depopulated molecular orbitals for predicting electronic excitation energies of valence, Rydberg, and charge-transfer states and potential energies near a conical intersection

Shaohong L. Li and Donald G. Truhlar

Citation: *The Journal of Chemical Physics* **141**, 104106 (2014); doi: 10.1063/1.4894522

View online: <http://dx.doi.org/10.1063/1.4894522>

View Table of Contents: <http://scitation.aip.org/content/aip/journal/jcp/141/10?ver=pdfcov>

Published by the **AIP Publishing**

Articles you may be interested in

[Performance of recent and high-performance approximate density functionals for time-dependent density functional theory calculations of valence and Rydberg electronic transition energies](#)

J. Chem. Phys. **137**, 244104 (2012); 10.1063/1.4769078

[A long-range-corrected density functional that performs well for both ground-state properties and time-dependent density functional theory excitation energies, including charge-transfer excited states](#)

J. Chem. Phys. **130**, 054112 (2009); 10.1063/1.3073302

[Excitation spectra of nitro-diphenylaniline: Accurate time-dependent density functional theory predictions for charge-transfer dyes](#)

J. Chem. Phys. **124**, 204321 (2006); 10.1063/1.2202735

[Time-dependent density-functional theory investigation of the formation of the charge transfer excited state for a series of aromatic donor-acceptor systems. Part II](#)

J. Chem. Phys. **117**, 4157 (2002); 10.1063/1.1498818

[Time-dependent density-functional theory investigation of the formation of the charge transfer excited state for a series of aromatic donor-acceptor systems. Part I](#)

J. Chem. Phys. **117**, 4146 (2002); 10.1063/1.1498817



COMSOL
CONFERENCE
2014 BOSTON

The Multiphysics
Simulation
Event of the Year



LEARN MORE >>

COMSOL

Testing time-dependent density functional theory with depopulated molecular orbitals for predicting electronic excitation energies of valence, Rydberg, and charge-transfer states and potential energies near a conical intersection

Shaohong L. Li and Donald G. Truhlar^{a)}

Department of Chemistry, Chemical Theory Center, and Supercomputing Institute, University of Minnesota, Minneapolis, Minnesota 55455, USA

(Received 8 July 2014; accepted 21 August 2014; published online 10 September 2014)

Kohn-Sham (KS) time-dependent density functional theory (TDDFT) with most exchange-correlation functionals is well known to systematically underestimate the excitation energies of Rydberg and charge-transfer excited states of atomic and molecular systems. To improve the description of Rydberg states within the KS TDDFT framework, Gaiduk *et al.* [Phys. Rev. Lett. **108**, 253005 (2012)] proposed a scheme that may be called HOMO depopulation. In this study, we tested this scheme on an extensive dataset of valence and Rydberg excitation energies of various atoms, ions, and molecules. It is also tested on a charge-transfer excitation of $\text{NH}_3\text{-F}_2$ and on the potential energy curves of NH_3 near a conical intersection. We found that the method can indeed significantly improve the accuracy of predicted Rydberg excitation energies while preserving reasonable accuracy for valence excitation energies. However, it does not appear to improve the description of charge-transfer excitations that are severely underestimated by standard KS TDDFT with conventional exchange-correlation functionals, nor does it perform appreciably better than standard TDDFT for the calculation of potential energy surfaces. © 2014 AIP Publishing LLC. [<http://dx.doi.org/10.1063/1.4894522>]

I. INTRODUCTION

Adiabatic Kohn-Sham (KS) linear-response (LR) time-dependent density functional theory (TDDFT),^{1,2} which we abbreviate as KS-LR in this paper, is the most widely used theory for the calculation of excitation energies of molecules. In principle it is a convenient, straightforward method that requires no more input than the specification of an approximate exchange-correlation functional and the specification of the molecular system. Especially when used with local exchange-correlation functionals [such as the local spin-density approximations (LSDA) or the generalized gradient approximations (GGA), which are sometimes called semilocal, but which are here called local since they depend only on local variables], it requires modest computational cost compared to reasonably accurate wave function theories (WFT) for excited states—like equation-of-motion coupled cluster (EOM-CC)³ theory or complete active space perturbation theory (CASPT)⁴—but gives comparable accuracy in many situations like the vertical excitation energies of valence states. There are well known cases, however, in which KS-LR with local approximate exchange-correlation functionals systematically fails.^{5,6} A particularly important case of the failures is that it underestimates Rydberg and long-range charge-transfer excitation energies by large margins. The reason is that local exchange-correlation potentials derived from the local functionals do not have the correct $-1/r$ behavior in the intermediate and

large- r (asymptotic) limits,⁷ where r is the distance between an electron and the remaining $(N - 1)$ -electron part of a N -electron system. Hybrid functionals, in which a percentage X of the local exchange is replaced by the non-local (Hartree-Fock) exchange, usually perform better but are still often not satisfactory.^{8–10}

Recently Staroverov and co-workers^{11,12} proposed an elegant scheme to improve the performance of KS-LR on Rydberg excitation energies without sacrificing the accuracy on valence excitation energies. They showed that, by depopulating a certain fraction of electrons from the KS highest occupied molecular orbital (HOMO), the behavior of the effective potential in the intermediate and asymptotic region can be made more accurate, and as a result the Rydberg excitation energies can be significantly improved. We will call this method “HOMO depopulation.” Although the method introduces a parameter δ (the number of electrons removed), the authors showed that the parameter depends on the exchange-correlation functional but optimized values “show relatively little system dependence” for the systems they tested. This is important for the wide applicability of the method and worth more validation.

In this paper, we will further test the performance of this HOMO depopulation method by considering a series of challenging systems, including valence, Rydberg, and charge-transfer excitations of atoms and molecules, and potential energy surfaces near a conical intersection. Instead of applying HOMO depopulation with full-linear-response KS-LR, we apply it with the Tamm-Dancoff approximation (TDA)^{13,14} to KS-LR,¹⁵ which we call KS-TDA. The reason for this is

^{a)} Author to whom correspondence should be addressed. Electronic mail: truhlar@umn.edu

that KS-TDA gives similar or even higher accuracy than KS-LR^{9,16} but is more stable near state intersections,⁵ which is especially desirable for calculations of potential energy surfaces for photochemical applications.

II. THEORY

Here, we give an overview of the method for closed-shell systems; for details, see Refs. 11 and 12. For a system with N electrons, Kohn-Sham density functional theory (KS-DFT) constructs a fictitious system with N non-interacting electrons that has the same electron density as the real system. The N non-interacting electrons occupy $N/2$ doubly-occupied KS molecular orbitals (MOs) which serve as input for the effective Hartree-exchange-correlation potential felt by the electrons. In the HOMO depopulation method, a total of δ electrons ($\delta/2$ α and $\delta/2$ β electrons, where δ is a real number between 0 and 2) are removed from the HOMO. If the HOMO is spatially M -fold degenerate, the δ electrons to be removed are evenly distributed among all degenerate HOMOs, namely, $(\delta/2M)$ α and $(\delta/2M)$ β electrons from each degenerate HOMO. The modified occupation numbers are used throughout the self-consistent field (SCF) procedure until convergence is reached. Then the converged KS orbitals are used in the subsequent KS-LR or KS-TDA calculations as if they are normal KS orbitals. The aim of this method is to make the effective potential closer to the exact potential in intermediate and asymptotic regions.

This method has a critical parameter δ that needs to be specified. In the original papers^{11,12} the authors showed that δ depends on the approximate exchange-correlation functional but is insensitive to choice of system among those they studied. Given an exchange-correlation functional, the method with a certain δ can significantly improve the excitation energies of Rydberg excited states while not sacrificing the accuracy for valence excited states. Here, we propose some more systematic and challenging tests for the method.

III. COMPUTATIONAL DETAILS

We implemented the HOMO depopulation method in a locally modified version of the GAMESS software package.¹⁷ It is used in the framework of KS-TDA with five functionals to calculate the electronic excitation energies of a series of systems and compare to reference values from experiment or high-level *ab initio* calculations. A grid of 99 radial shells and 590 angular points per shell is used for numerical integration for all the DFT-based methods.

The dataset of valence and Rydberg excitation energies of atoms includes eight valence and 16 Rydberg excitation energies of six closed-shell atoms and atomic ions (Be, B⁺, Ne, Na⁺, Mg, Al⁺) as used in Ref. 10. This database may be called AEE24 (denoting 24 atomic excitation energies); it contains the two lowest singlet singly excited states and two lowest triplet singly excited states of each atom and ion. "Singly-excited" means only one electron is excited from the closed shell to a higher atomic orbital shell. For Be, B⁺, Mg, and Al⁺, the lowest singlet and triplet singly-excited states are valence states and the second lowest states are Rydberg

states, while for Ne and Na⁺ all excited states are Rydberg states. The basis sets used are: aug-cc-pVQZ^{18,19} for Be and B⁺, d-aug-cc-pVQZ^{18,19} for Ne, aug-cc-pCVQZ²⁰ for Na⁺, and aug-cc-pV(Q+d)Z^{18,19,21} for Mg and Al⁺, following Ref. 10.

The dataset of molecules includes 30 valence and 39 Rydberg excitation energies of 11 closed-shell organic molecules (acetaldehyde, acetone, ethylene, formaldehyde, isobutene, pyrazine, pyridazine, pyridine, pyrimidine, s-tetrazine, t-butadiene) as used in Ref. 9. This database may be called MEE69 (denoting 69 molecular excitation energies). The geometries of all the molecules are also taken from Ref. 9. For molecules it is not always clear if an excited state is valence or Rydberg, and here we use the same judgments already made in Ref. 9. Another ambiguity is in the assignment of the calculated states since KS-LR and KS-TDA tend to over-stabilize Rydberg and charge-transfer states, bringing some uninteresting high-energy states down to the low-energy spectrum of interest. We choose to line up the states in energy order within each irreducible representation, also following Ref. 9. The reason and a discussion of other possible assignments can be found in the same reference. The 6-31(2+,2+)G(d,p)²² basis set is used for all the molecules. This basis set is flexible enough that the error from the limited size of the basis set is minor compared to the error from the approximate functional used with KS-TDA.

The functionals used in the test of valence and Rydberg states include an LSDA functional, namely, GVVN5 (also known as SVWN5),²³ a GGA functional, namely, BLYP,^{24,25} three hybrid functionals, namely, B3LYP²⁶ (which has $X = 20$, where X is the percentage of Hartree-Fock exchange), M06^{27,28} ($X = 27$), and M06-2X^{27,28} ($X = 54$). (See the supplementary material for some comments on B3LYP in GAMESS.²⁹) We choose only these five representative functionals instead of a large variety because the purpose of this paper is to test the HOMO depopulation correction to KS-TDA rather than testing the functionals.

Note that some researchers, especially physicists, call GGAs semilocal, whereas many others, especially chemists, label any energy density functional that depends only on local variables, such as the local density, the local density gradient, or the local kinetic energy density, as local; a local functional should not be confused with a local-density functional, which depends only on the local density, not on other local variables. The Hartree-Fock energy density is labeled as nonlocal because, like the Coulomb energy density (sometimes called the Hartree term, especially by physicists), it involves an integral over all space.

For some calculations we also consider a database with 46 diverse data; this database will be called DEE46 (46 diverse excitation energies). This contains the eight valence excitation energies (four singlet and four triplet) and 16 Rydberg excitation energies (eight singlet and eight triplet) of AEE24, the four valence and eight Rydberg singlet-triplet splittings from corresponding pairs of excitation energies in AEE24, and ten valence singlet excitation energies from MEE69. The ten singlet excitation energies are the lowest-energy valence singlet excitation energies of each of the ten molecules that have valence excitations (isobutene has no valence

TABLE I. Mean signed errors (MSE) and mean unsigned errors (MUE) over the eight valence states, 16 Rydberg states, and all 24 excited states of the six atoms and atomic ions as calculated by KS-TDA with HOMO depopulation with five functionals. The functionals are listed in order of increasing overall MUE with the optimum δ (which is shown in bold face).

Exchange-correlation functionals	δ	MSE (eV)			MUE (eV)		
		Valence	Rydberg	All	Valence	Rydberg	All
B3LYP	0	-0.13	-1.89	-1.30	0.22	1.89	1.33
	0.15	-0.12	-0.68	-0.50	0.28	0.69	0.55
	0.2	-0.13	-0.29	-0.23	0.31	0.34	0.33
	0.25	-0.13	0.11	0.03	0.35	0.23	0.27
	0.3	-0.14	0.51	0.29	0.38	0.51	0.47
BLYP	0	-0.11	-2.70	-1.84	0.23	2.70	1.88
	0.15	0.03	-1.36	-0.89	0.27	1.36	1.00
	0.2	0.07	-0.91	-0.58	0.31	0.96	0.74
	0.25	0.11	-0.46	-0.27	0.36	0.60	0.52
	0.3	0.15	-0.02	0.03	0.40	0.35	0.37
	0.35	0.18	0.41	0.34	0.44	0.47	0.46
	0.4	0.21	0.86	0.64	0.48	0.86	0.73
M06	0	-0.20	-2.50	-1.73	0.23	2.50	1.75
	0.15	-0.20	-1.31	-0.94	0.23	1.31	0.95
	0.2	-0.20	-0.91	-0.67	0.24	0.91	0.69
	0.25	-0.21	-0.51	-0.41	0.25	0.53	0.44
	0.3	-0.22	-0.12	-0.15	0.27	0.44	0.38
	0.35	-0.24	0.27	0.10	0.28	0.55	0.46
	0.4	-0.25	0.66	0.36	0.30	0.80	0.63
GVWN5	0	0.00	-2.29	-1.53	0.17	2.29	1.58
	0.15	0.14	-0.93	-0.57	0.25	1.01	0.75
	0.2	0.18	-0.47	-0.25	0.29	0.64	0.53
	0.25	0.22	-0.03	0.06	0.33	0.40	0.38
	0.3	0.25	0.42	0.37	0.37	0.46	0.43
M06-2X	0	0.09	-1.21	-0.78	0.27	1.21	0.90
	0.05	0.04	-0.87	-0.57	0.30	0.87	0.68
	0.1	-0.02	-0.54	-0.37	0.33	0.57	0.49
	0.15	-0.08	-0.22	-0.18	0.37	0.50	0.46
	0.2	-0.15	0.10	0.02	0.43	0.51	0.48
	0.25	-0.22	0.42	0.20	0.48	0.63	0.58
	0.3	-0.30	0.74	0.39	0.54	0.87	0.76

excitations). The diverse database has 22 valence data and 24 Rydberg data.

The test of charge-transfer excitation is chosen to be the ${}^3A_1 [n(N) \rightarrow \sigma^*(F_2)]$ excitation of the NH_3-F_2 complex. The geometry of the complex is taken from Ref. 30. In particular, the intermolecular distance of NH_3 and F_2 is 6 Å. The functional and basis set used for this calculation is B3LYP/6-31+G(d,p).³¹

The potential energy curves near a conical intersection between the ground and the first excited states of NH_3 are also tested. The geometries are taken to be planar, with all $\angle HNH = 60^\circ$, $r(N-H_B) = r(N-H_C) = 1.020$ Å, and $r(N-H_A)$ is the coordinate along which the potential energy curves are calculated. The reference multi-configurational quasi-degenerate perturbation theory (MC-QDPT) calculations³² gave a symmetry-allowed conical intersection at $r(N-H_A) = 2.0-2.1$ Å. The functional and basis set for this calculation is B3LYP/6-311+G(3df, 3pd).³³

In order to place the results in perspective, we also report comparisons to spin-flip TDDFT, in both its collinear³⁴ and

noncollinear^{10,35} versions. We sometimes abbreviate “spin-flip” as SF.

IV. RESULTS AND DISCUSSION

IV.A. Valence and Rydberg excitations

The mean signed error (MSE) and mean unsigned error (MUE) of the valence and Rydberg states and of all of the excitation energies of all the atoms and molecules, as compared to the reference values, are summarized in Tables I and II, respectively. (The supplementary material gives a representative set of data that may be useful by researchers who want to check some of the calculations.²⁹)

As is well known, standard KS-TDA ($\delta = 0$) with many exchange-correlation functionals gives rather accurate valence excitation energies but significantly underestimates Rydberg excitation energies, giving a large MUE for Rydberg excitation energies and a negative MSE with similar magnitude. As δ increases, the Rydberg excitation energies increase monotonically, their MSE goes from negative to positive, and

TABLE II. Mean signed errors (MSE) and mean unsigned errors (MUE) over the 30 valence states, 39 Rydberg states, and all 69 excited states of the 11 molecules as calculated by KS-TDA HOMO depopulation with five functionals. The functionals are listed in order of increasing overall MUE with the optimum δ (which is shown in bold face).

Exchange-correlation functionals	δ	MSE (eV)			MUE (eV)		
		Valence	Rydberg	All	Valence	Rydberg	All
B3LYP	0	0.09	-0.85	-0.44	0.25	0.86	0.59
	0.15	0.17	-0.23	-0.05	0.26	0.30	0.28
	0.2	0.19	-0.04	0.06	0.27	0.16	0.21
	0.25	0.20	0.16	0.18	0.28	0.21	0.24
	0.3	0.21	0.36	0.30	0.29	0.37	0.34
BLYP	0	-0.41	-1.54	-1.05	0.48	1.54	1.08
	0.15	-0.17	-0.75	-0.50	0.33	0.77	0.58
	0.2	-0.10	-0.48	-0.31	0.30	0.51	0.42
	0.25	-0.04	-0.21	-0.14	0.29	0.28	0.29
	0.3	0.01	0.04	0.03	0.29	0.18	0.23
	0.35	0.05	0.23	0.15	0.29	0.28	0.29
	0.4	0.08	0.45	0.29	0.29	0.49	0.41
M06	0	-0.10	-1.28	-0.77	0.27	1.28	0.84
	0.15	0.04	-0.75	-0.41	0.25	0.75	0.53
	0.2	0.06	-0.54	-0.28	0.24	0.56	0.42
	0.25	0.08	-0.34	-0.15	0.24	0.39	0.32
	0.3	0.10	-0.15	-0.05	0.25	0.28	0.27
	0.35	0.11	0.03	0.06	0.26	0.29	0.28
	0.4	0.11	0.20	0.16	0.27	0.36	0.32
GVWN5	0	-0.42	-1.22	-0.87	0.53	1.23	0.92
	0.15	-0.19	-0.42	-0.32	0.40	0.47	0.44
	0.2	-0.13	-0.17	-0.15	0.38	0.28	0.32
	0.25	-0.08	0.08	0.01	0.38	0.22	0.29
	0.3	-0.05	0.30	0.15	0.38	0.36	0.37
M06-2X	0	0.36	-0.17	0.06	0.45	0.29	0.36
	0.05	0.34	-0.04	0.12	0.46	0.23	0.33
	0.1	0.32	0.08	0.19	0.46	0.23	0.33
	0.15	0.29	0.19	0.24	0.46	0.27	0.35
	0.2	0.27	0.31	0.29	0.47	0.35	0.40
	0.25	0.23	0.39	0.32	0.46	0.41	0.43
	0.3	0.20	0.48	0.36	0.47	0.49	0.48

their MUE first decreases then increases, giving a minimum. Our calculations show that MUE for Rydberg excitation energies can be significantly reduced from >1 eV to as small as 0.2 eV.

On the other hand, the MSE and MUE of valence excitation energies do not have a general trend. For atoms, the valence MUE usually increases as δ increases; for molecules, it can be larger or smaller as δ increases, depending on the functional. Regardless of it being larger or smaller, however, the difference with $\delta = 0$ and with the optimal δ (giving smallest overall MUE) is usually less than 0.2 eV, which means the valence excitation energies are less sensitive to δ than the Rydberg excitation energies are. Consequently, the overall MUE can be reduced with a functional-dependent δ .

Among the five tested functionals, B3LYP with $\delta = 0.25$ has the best performance for the atoms and ions (overall MUE = 0.27 eV). Xu *et al.*¹⁰ have done extensive tests of various schemes of linear-response TDDFT, including KS-LR, KS-TDA, and spin-flip TDDFT³⁶ in the Tamm-Dancoff approximation (abbreviated as SF-TDA hereafter) on the same

dataset of atoms and ions. In addition to the four excitation energies for each atom and ion, they included two singlet-triplet splittings for each atom and ion in the statistics as well. Including the two splittings so we can compare to that work, the best result for the present work is an overall MUE = 0.25 eV from B3LYP with $\delta = 0.25$. In comparison, the best result of Ref. 10 is an overall MUE of 0.27 eV from a noncollinear^{10,35} scheme [in particular “N-EA-SPQ:GVWN5” (See Ref. 10 for the meaning of this notation.)] Thus, we find that the best result of the current test outperforms the best result of the article by Xu *et al.*¹⁰ Table III organizes the results from the five functionals with the best tested δ , the top five SF-TDA methods of Xu *et al.*, the top five KS-TDA methods tested in the article of Xu *et al.* and in this work, and two WFT methods. Xu *et al.* have shown that SF-TDA with a noncollinear kernel, when interpreted carefully, has better overall performance than standard KS-LR and KS-TDA for this database. Here, Table III shows that the HOMO depopulation method with selected functionals and proper δ is competitive with the best SF-TDA methods and even with CASPT2 (complete active

TABLE III. Mean unsigned errors (MUE, in eV) over the 12 valence excitations and singlet-triplet splittings, 24 Rydberg excitations and singlet-triplet splittings, and all 36 excitations and singlet-triplet splittings of the six atoms and atomic ions. Five of the HOMO depopulation calculations, the best five noncollinear spin-flip methods of Ref. 10, the best five KS-TDA methods of Ref. 10 and this work, and two WFT methods are listed for comparison. The methods are listed in order of increasing overall MUE.

Method	Valence	Rydberg	Overall	Reference
EOM-CCSD	0.04	0.12	0.09	Ref. 10
CASPT2	0.12	0.30	0.24	Ref. 10
KS-TDA B3LYP ($\delta = 0.25$)	0.41	0.18	0.25	This work
N-EA-S12:GVWN5	0.24	0.28	0.27	Ref. 10
KS-TDA M06 ($\delta = 0.3$)	0.25	0.33	0.30	This work
KS-TDA GVWN5 ($\delta = 0.25$)	0.34	0.31	0.32	This work
KS-TDA BLYP ($\delta = 0.3$)	0.46	0.27	0.33	This work
N-OA-S12:M06	0.33	0.33	0.33	Ref. 10
KS-TDA M06-2X ($\delta = 0.15$)	0.33	0.36	0.35	This work
N-EA-S12:B3PW91	0.46	0.32	0.37	Ref. 10
N-EA-S22:LRC- ω PBE	0.64	0.25	0.38	Ref. 10
N-EA-S22:LRC- ω PBEh	0.69	0.27	0.41	Ref. 10
KS-TDA M06-2X	0.27	0.83	0.64	Ref. 10
KS-TDA ω B97X	0.17	1.11	0.80	Ref. 10
KS-TDA B97-1	0.11	1.18	0.82	Ref. 10
KS-TDA B3PW91	0.30	1.14	0.86	Ref. 10
KS-TDA B3LYP	0.24	1.29	0.94	This work

space perturbation theory of second order) for this database. In comparison, the best standard KS-TDA methods are outperformed by a wide margin.

For the organic molecules, we observed similar trends as for the atoms. B3LYP with $\delta = 0.2$ has the best performance (overall MUE = 0.21 eV). Isegawa *et al.*⁹ have tested KS-LR with various exchange-correlation functionals on the same dataset of molecular excitations, and the best result they obtained is overall MUE = 0.30 eV from M06-2X, which is outperformed by the best result here by a wide margin. Table IV organizes the results for the five functionals for the HOMO depopulation method, each with its optimum tested δ , for the same five functionals with standard KS-TDA ($\delta = 0$), for the top five KS-LR methods of Isegawa *et al.*, and for one WFT method (EOM-CCSD). Four of the five listed KS-TDA methods with HOMO depopulation outperform the best KS-LR methods, and two even outperform EOM-CCSD for this database, although the difference in performance is not as significant as for the database of atoms. The standard KS-TDA methods in Table IV are generally not as good as the KS-LR methods, but we need to be aware that the listed functionals for KS-LR are the top five out of the 30 functionals tested by Isegawa *et al.*, whereas the five functionals for KS-TDA are only a representative set of the popular types of functionals used for testing HOMO depopulation in this work.

To give a more comprehensive comparison among the various TDDFT schemes (KS-LR, KS-TDA, KS-TDA with HOMO depopulation, and collinear and noncollinear SF-TDA), we made additional tests employing the DEE46 database. Two widely used functionals that have good general performance, M06 and B3LYP, are tested on this dataset with the various kinds of TDDFT schemes. The mean un-

TABLE IV. Mean unsigned errors (MUE, in eV) over the 30 valence states, 39 Rydberg states, and all 69 excited states of the 11 molecules. Five of the HOMO depopulation calculations, five standard KS-TDA calculations ($\delta = 0$) with the same functionals, the best five KS-LR methods of Ref. 9, and a WFT method (EOM-CCSD) are listed for comparison. The methods are listed in order of increasing overall MUE.

Method	Valence	Rydberg	Overall	Reference
KS-TDA B3LYP ($\delta = 0.2$)	0.27	0.16	0.21	This work
KS-TDA BLYP ($\delta = 0.3$)	0.29	0.18	0.23	This work
KS-TDA M06 ($\delta = 0.3$)	0.25	0.28	0.27	This work
EOM-CCSD	0.47	0.11	0.27	Ref. 9
KS-TDA GVWN5 ($\delta = 0.25$)	0.38	0.22	0.29	This work
KS-LR M06-2X	0.36	0.26	0.30	Ref. 9
KS-LR ω B97X-D	0.32	0.28	0.30	Ref. 9
KS-LR MPWKCS1K	0.40	0.27	0.32	Ref. 9
KS-LR PWB6K	0.43	0.24	0.32	Ref. 9
KS-TDA M06-2X ($\delta = 0.1$)	0.46	0.23	0.33	This work
KS-LR CAM-B3LYP	0.31	0.35	0.33	Ref. 9
KS-TDA M06-2X	0.45	0.29	0.36	This work
KS-TDA B3LYP	0.25	0.86	0.59	This work
KS-TDA M06	0.27	1.28	0.84	This work
KS-TDA GVWN5	0.53	1.23	0.92	This work
KS-TDA BLYP	0.48	1.54	1.08	This work

signed errors are organized in Table V. Table V shows that for the two functionals studied, the ranking of overall MUE is (best) KS-TDA with HOMO depopulation, (second best) noncollinear SF-TDA, (third) collinear SF-TDA, (fourth) KS-TDA, and (fifth) KS-LR, which is consistent with the trends in Tables III and IV. Standard KS-TDA gives satisfactory accuracy for valence excitations but is poor for predicting Rydberg excitations, while KS-TDA with HOMO depopulation and SF-TDA strike a much better balance between the accuracy of the two types of excitations. We remind the reader that, although SF-TDA can give good results for both valence

TABLE V. Mean unsigned errors (MUE, in eV) of KS-TDDFT methods over the DEE46 database of atomic and molecular excitation energies and spin splittings.^a

Method	Valence	Rydberg	Overall	Reference
HOMO-depopulated TDA B3LYP ^b	0.31	0.16	0.23	This work
HOMO-depopulated TDA M06 ^c	0.20	0.31	0.26	This work
Noncollinear spin-flip TDA M06 ^d	0.36	0.33	0.35	Refs. 10 and 36
Collinear spin-flip TDA M06 ^e	0.40	0.68	0.54	Refs. 10 and 36
TDA B3LYP	0.19	1.29	0.77	This work
LR B3LYP	0.32	1.30	0.83	This work, Ref. 36
TDA M06	0.22	1.71	1.00	This work
LR M06	0.35	1.72	1.07	Refs. 10 and 36

^aThe methods are listed in order of increasing overall MUE.

^b $\delta = 0.25$.

^c $\delta = 0.3$.

^dRecalculated from the "N-OA-S12:M06" data of Ref. 10 and the "NC-NSF2 M06" data of Ref. 36.

^eRecalculated from the "C-EA-S11:M06" data of Ref. 10 and the "NSF2 M06" data of Ref. 36.

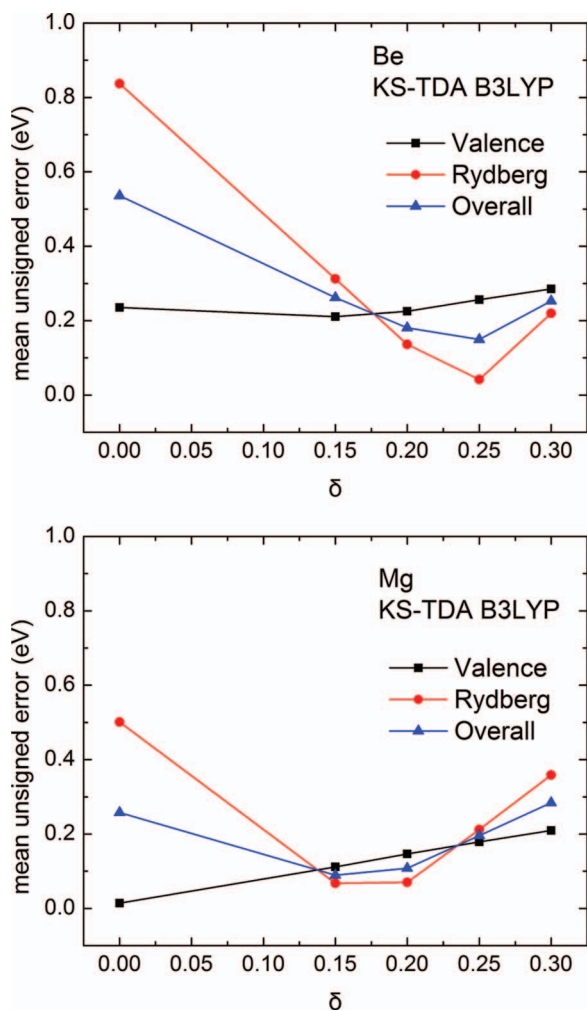


FIG. 1. Mean unsigned error (MUE) over the two valence excitations, over the two Rydberg excitations, and over all four excitations of Be (top) and Mg (bottom) as a function of δ calculated by KS-TDA B3LYP with HOMO depopulation (Basis set: aug-cc-pVQZ for Be and aug-cc-pV(Q+d)Z for Mg).

and Rydberg excitations, it has several subtleties and must be used with caution (for how the subtleties can significantly affect the accuracy of SF-TDA, we refer the interested reader to the discussions in Refs. 10 and 36). In contrast, KS-TDA with HOMO depopulation is simple to use, with only one parameter δ to be determined (or one can use the recommended δ values of Table V).

Note that we have chosen only several discrete δ values for testing instead of fully optimizing the value of δ , because our aim is to study the effect of δ and the general performance rather than finding the absolutely optimal δ . Furthermore, we do not need to find the overall optimal δ since the general usefulness of the method is due to the fact that the performance can be improved within a range of δ (as opposed to a tightly optimized specific value of δ) that applies to all atoms and molecules tested, as described next.

In the first papers in the HOMO depopulation method^{11,12} the authors showed that the proper value of δ has weak system dependence. This finding can be further elaborated by examination of our tests. For instance, we can compare the error of excitation energies of Be and Mg calculated

by KS-TDA with B3LYP, as Fig. 1 shows. Evidently, the optimal δ for valence and Rydberg excitations, or for Be and Mg, is rather different: for Be, the optimal tested δ for valence states is 0.15, and for Rydberg states it is 0.25, while for Mg, the optimal tested δ for valence states is 0, and for Rydberg states it is 0.15. Nevertheless, if we take a compromise value of 0.2 for both, we can get an overall MUE of 0.1–0.2 eV, which is much better than the MUE for the original $\delta = 0$. In fact, the Rydberg excitations are improved by a greater amount than the amount by which the valence excitations are worsened, and δ does not need to be at its very optimal value to improve the overall performance. This is the key advantage that makes this method useful: the overall performance can be significantly better than the standard KS-TDA in a rather wide range of δ which depends only weakly on the system under study.

Staroverov and co-workers^{11,12} showed that hybrid functionals need smaller corrections than local functionals do. This trend also shows up in this study, though not strictly so. The two local functionals, GVWN5 and BLYP, achieve best performance at $\delta = 0.25$ and 0.3 , respectively, for both the atoms and the molecules. The behavior of the hybrid functionals is diverse: M06-2X needs $\delta = 0.15$ and 0.1 for best performance on atoms and molecules, respectively, B3LYP needs 0.25 and 0.2 , and M06 needs 0.3 for both. Comparing the performance of the standard ($\delta = 0$) KS-TDA with local and hybrid functionals, it is clear that those that originally perform better need less correction. Hybrid functionals, especially those like M06-2X with a high percentage of Hartree-Fock exchange, usually have better performance for Rydberg excitation energies because of the better asymptotic behavior of the Hartree-Fock exchange potential. On the other hand, M06, despite its hybrid nature, needs larger δ . In summary, we find that how large of a δ is needed is directly related to the performance of the original functional: functionals that perform better without HOMO depopulation need smaller δ .

IV.B. Charge-transfer excitation of $\text{NH}_3\text{-F}_2$

The success of the method on Rydberg states can be ascribed to a more accurate Hartree-exchange-correlation potential in the intermediate and near-asymptotic region.^{11,12} On the other hand, the performance on long-range charge-transfer excitations depends on the asymptotic behavior of the potential at even larger r . The ${}^3A_1 n(\text{N}) \rightarrow \sigma^*(\text{F}_2)$ excitation of $\text{NH}_3\text{-F}_2$, in which the intermolecular distance of the two monomers is 6 \AA , represents an extreme and clear case of long-range charge-transfer excitation.²⁷ The reason for this is that it is a long-range charge transfer state with negligible overlap of the charge distributions of the subsystems.^{37,38}

KS-TDA with B3LYP/6-31+G(d,p) substantially underestimates the excitation energy, giving 2.22 eV compared to the reference symmetry-adapted-cluster configuration interaction (SAC-CI) value 9.46 eV .³⁰ As Fig. 2 shows, HOMO depopulation raises the excitation energy (as it does for Rydberg excitations), but the δ needed to reach the correct level is $0.8\text{--}0.9$, much larger than the appropriate value for valence and Rydberg excitations in our previous test ($0.2\text{--}0.25$). The δ

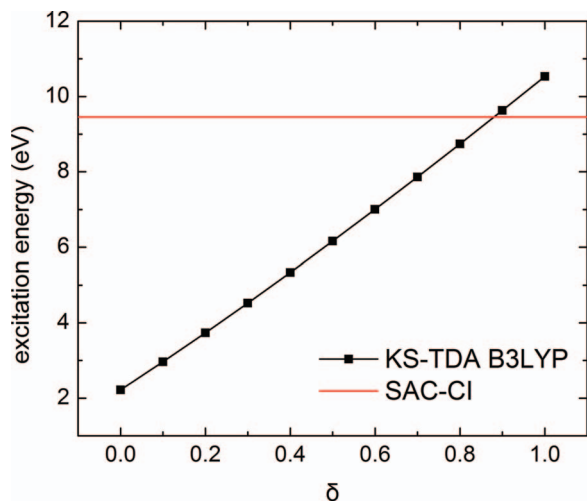


FIG. 2. The excitation energy of the 3A_1 charge-transfer state of $\text{NH}_3\text{-F}_2$ calculated by KS-TDA B3LYP/6-31+G(d,p) with HOMO depopulation as a function of δ (black line with solid squares), and the reference SAC-CI/6-31+G(d,p) value taken from Zhao and Truhlar²⁷ (red horizontal line).

value needed to correct the asymptotic region of the potential is much larger than that needed to correct the intermediate region, and one cannot get good results for both simultaneously.

IV.C. Potential energy curves of NH_3 near a conical intersection

So far we have considered only excitations at single geometries. This is important for spectroscopy, but to extend further the applicability of the method to photochemistry, we need to test its performance on potential energy surfaces at geometries far from equilibrium. Conical intersections are especially challenging cases and are critical for applications of photochemistry. One challenge is that KS-TDA gives $F - 1$ instead of the correct $F - 2$ dimensions for conical intersections of the KS-DFT reference state and a response state,³⁹⁻⁴¹ where F is the internal degrees of freedom of the system. This can be remedied by the recently proposed CIC-TDA method,⁴² but for simplicity we here choose to study a symmetry-allowed conical intersection of NH_3 that does not have this complexity.

The potential energy curves are plotted in Fig. 3. Compared to the reference MC-QDPT results,³² standard KS-TDA with B3LYP overestimates both the ground and the first singlet excited states by as large as 1–2 eV, and the intersection appears at longer N– H_A distance. The HOMO depopulation correction with $\delta = 0.25$ brings down both curves by ~ 0.1 eV, making them closer to the reference curves but still far from acceptable. Even if we assume that the curves would keep moving down as δ keeps increasing, it would need much too large of a δ to make the curves reasonable, in particular so large that the excitations near the equilibrium geometry would no longer be accurate.

Another point related to potential energy surfaces that is worth noting is that the HOMO depopulation method is not size consistent. If the energies of two different non-interacting molecular motifs are calculated individually, the HOMO of

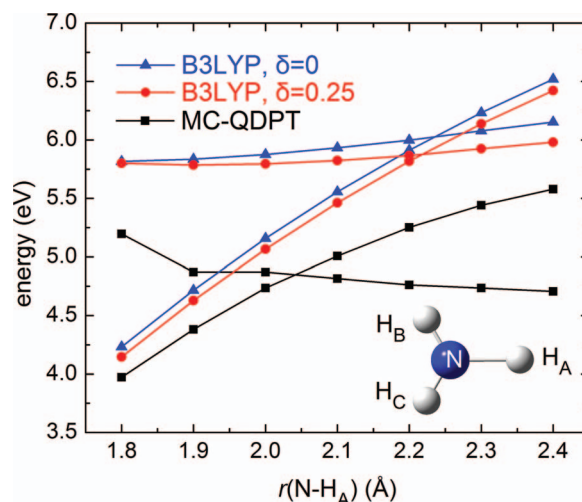


FIG. 3. The potential energy curves of the S_0 and S_1 states of NH_3 near a conical intersection calculated by KS-TDA B3LYP/6-311+G(3df,3pd) with ($\delta = 0.25$) and without ($\delta = 0$) HOMO depopulation, and the reference MC-QDPT results taken from Ref. 32.

both will be depopulated, but if they are put together and the total energy is calculated, only the HOMO of one of them will be depopulated. The lack of size consistency limits the application of the method for problems like the calculation of potential energy surfaces of chemical reactions or photodissociation.

IV.D. Further discussion

Figure 2 also manifests an interesting phenomenon in that the excitation energy of the state changes almost linearly with δ in a wide range of δ . In fact, this happens for almost all the tests carried out in this study, regardless of the character (valence or Rydberg or charge-transfer) of the state. Generally the slope of the excitation energy versus δ curve is considerably larger for Rydberg and charge-transfer states than for valence states. The slope for valence states can be positive or negative, while for most Rydberg and charge-transfer states it is positive. Since KS-LR and KS-TDA with conventional local and hybrid functionals systematically underestimate the excitation energies of Rydberg states while giving reasonable excitation energies of valence states, HOMO depopulation with a proper δ can achieve a good compromise for the accuracy of valence states and Rydberg states if the underestimation of Rydberg excitation is not too severe. In contrast, if the underestimation of a state energy is very large, as in the $\text{NH}_3\text{-F}_2$ case in this study, the large δ needed to obtain reasonable accuracy of the state may ruin the accuracy of the other states.

V. CONCLUSIONS

We have tested the HOMO depopulation method proposed by Staroverov and co-workers^{11,12} with the linear-response Kohn-Sham time-dependent density functional theory in the Tamm-Dancoff approximation (KS-TDA) on the valence, Rydberg, and charge-transfer excitation energies of

a variety of atomic and molecular systems, as well as the potential energy curves of NH_3 near a conical intersection. With the tested local or hybrid functionals and a properly chosen parameter δ , the method is able to improve the excitation energies of Rydberg states while preserving reasonable accuracy of valence excitation energies. Improved overall performance for the tested valence and Rydberg states can be achieved in a wide range of δ independent of the systems.

For the severely underestimated charge-transfer state of $\text{NH}_3\text{-F}_2$, however, the δ needed to obtain reasonable accuracy is much larger than the value for valence and Rydberg states, and the method may not be very useful in this situation. The method does not improve much the potential energy curves of NH_3 near a conical intersection, and due to the lack of size extensivity the method is not suitable for the calculation of potential energy surfaces for chemical and photochemical reactions. This is not surprising since the HOMO depopulation method is essentially an asymptotic correction to the KS potential, and this alone cannot solve all the problems of local and hybrid functionals. In summary, we conclude that the HOMO depopulation method is very promising, and we highly recommended it for spectroscopic calculations involving both valence and Rydberg states but not for calculations of long-range charge transfer states or potential energy surfaces.

ACKNOWLEDGMENTS

The authors are grateful to Xuefei Xu and Aleksandr V. Marenich for very helpful assistance. We are also grateful to Alex Gaiduk and Viktor Staroverov for stimulating discussion and helpful correspondence. This work was supported in part by the U. S. Department of Energy, Office of Basic Energy Sciences, under Grant No. DE-SC0008666.

- ¹M. A. L. Marques and E. K. U. Gross, *Annu. Rev. Phys. Chem.* **55**, 427 (2004).
- ²M. E. Casida, in *Recent Advances in Density Functional Methods, Part I*, edited by D. P. Chong (World Scientific, Singapore, 1995), pp. 155.
- ³I. Shavitt and R. J. Bartlett, *Many-Body Methods in Chemistry and Physics* (Cambridge University Press, 2009).
- ⁴K. Andersson, P. A. Malmqvist, and B. O. Roos, *J. Chem. Phys.* **96**, 1218 (1992).
- ⁵M. E. Casida and M. Huix-Rotllant, *Annu. Rev. Phys. Chem.* **63**, 287 (2012).
- ⁶L. González, D. Escudero, and L. Serrano-Andrés, *ChemPhysChem* **13**, 28 (2012).
- ⁷M. E. Casida, C. Jamorski, K. C. Casida, and D. R. Salahub, *J. Chem. Phys.* **108**, 4439 (1998).
- ⁸M. Caricato, G. W. Trucks, M. J. Frisch, and K. B. Wiberg, *J. Chem. Theory Comput.* **6**, 370 (2010).

- ⁹M. Isegawa, R. Peverati, and D. G. Truhlar, *J. Chem. Phys.* **137**, 244104 (2012).
- ¹⁰X. Xu, K. R. Yang, and D. G. Truhlar, *J. Chem. Theory Comput.* **10**, 2070 (2014).
- ¹¹A. P. Gaiduk, D. S. Firaha, and V. N. Staroverov, *Phys. Rev. Lett.* **108**, 253005 (2012).
- ¹²A. P. Gaiduk, D. Mizzi, and V. N. Staroverov, *Phys. Rev. A* **86**, 052518 (2012).
- ¹³J. Tamm, *J. Phys. (Moscow)* **9**, 449 (1945).
- ¹⁴S. M. Dancoff, *Phys. Rev.* **78**, 382 (1950).
- ¹⁵S. Hirata and M. Head-Gordon, *Chem. Phys. Lett.* **314**, 291 (1999).
- ¹⁶A. D. Laurent and D. Jacquemin, *Int. J. Quantum Chem.* **113**, 2019 (2013).
- ¹⁷M. W. Schmidt, K. K. Baldrige, J. A. Boatz, S. T. Elbert, M. S. Gordon, J. H. Jensen, S. Koseki, N. Matsunaga, K. A. Nguyen, S. J. Su, T. L. Windus, M. Dupuis, and J. A. Montgomery, *J. Comput. Chem.* **14**, 1347 (1993); M. S. Gordon and M. W. Schmidt, in *Theory and Applications of Computational Chemistry: The First Forty Years*, edited by C. E. Dykstra, G. Frenking, K. S. Kim, and G. E. Scuseria (Elsevier, Amsterdam, 2005), pp. 1167–1189.
- ¹⁸J. T. H. Dunning, *J. Chem. Phys.* **90**, 1007 (1989).
- ¹⁹D. E. Woon and J. T. H. Dunning, *J. Chem. Phys.* **98**, 1358 (1993).
- ²⁰See <https://bse.pnl.gov/bse/portal>; accessed 24 March 2014.
- ²¹T. H. Dunning, K. A. Peterson, and A. K. Wilson, *J. Chem. Phys.* **114**, 9244 (2001).
- ²²K. B. Wiberg, A. E. de Oliveira, and G. Trucks, *J. Phys. Chem. A* **106**, 4192 (2002).
- ²³P. A. M. Dirac, *Proc. Cambridge Philos. Soc.* **26**, 376 (1930); R. Gáspár, *Acta Physiol. Acad. Sci. Hung.* **3**, 263 (1954); **35**, 213 (1974); S. H. Vosko, L. Wilk, and M. Nusair, *Can. J. Phys.* **58**, 1200 (1980).
- ²⁴A. D. Becke, *Phys. Rev. A* **38**, 3098 (1988).
- ²⁵C. T. Lee, W. T. Yang, and R. G. Parr, *Phys. Rev. B* **37**, 785 (1988).
- ²⁶P. J. Stephens, F. J. Devlin, C. F. Chabalowski, and M. J. Frisch, *J. Phys. Chem.* **98**, 11623 (1994).
- ²⁷Y. Zhao and D. G. Truhlar, *Theor. Chem. Acc.* **120**, 215 (2008).
- ²⁸Y. Zhao and D. G. Truhlar, *Acc. Chem. Res.* **41**, 157 (2008).
- ²⁹See supplementary material at <http://dx.doi.org/10.1063/1.4894522> for a representative set of the calculated valence and Rydberg excitation energies of the atoms and molecules and comments on the B3LYP functional used in GAMESS.
- ³⁰Y. Zhao and D. G. Truhlar, *J. Phys. Chem. A* **110**, 13126 (2006).
- ³¹W. J. Hehre, R. Ditchfield, and J. A. Pople, *J. Chem. Phys.* **56**, 2257 (1972).
- ³²S. Nangia, D. G. Truhlar, M. J. McGuire, and P. Piecuch, *J. Phys. Chem. A* **109**, 11643 (2005).
- ³³R. Krishnan, J. S. Binkley, R. Seeger, and J. A. Pople, *J. Chem. Phys.* **72**, 650 (1980).
- ³⁴Y. Shao, M. Head-Gordon, and A. I. Krylov, *J. Chem. Phys.* **118**(11), 4807 (2003).
- ³⁵F. Wang and T. Ziegler, *J. Chem. Phys.* **121**, 12191 (2004); **122**, 074109 (2005); *Int. J. Quantum Chem.* **106**, 2545 (2006).
- ³⁶M. Isegawa and D. G. Truhlar, *J. Chem. Phys.* **138**, 134111 (2013).
- ³⁷M. J. G. Peach, P. Benfield, T. Helgaker, and D. J. Tozer, *J. Chem. Phys.* **128**, 044118 (2008).
- ³⁸R. Li, J. Zheng, and D. G. Truhlar, *Phys. Chem. Chem. Phys.* **12**, 12697 (2010).
- ³⁹H. C. Longuet-Higgins, *Proc. R. Soc. London, Ser. A* **344**, 147 (1975).
- ⁴⁰C. A. Mead, *J. Chem. Phys.* **70**, 2276 (1979).
- ⁴¹B. G. Levine, C. Ko, J. Quenneville, and T. J. Martínez, *Mol. Phys.* **104**, 1039 (2006).
- ⁴²S. L. Li, A. V. Marenich, X. Xu, and D. G. Truhlar, *J. Phys. Chem. Lett.* **5**, 322 (2014).